Isobutane dehydrogenation over high-performanced sulfide V-K/γ-Al 2 O 3 catalyst: modulation of vanadium species and intrinsic effect of potassium

Yu-Peng Tian, Xin-Mei Liu, Svetlana Mintova, Long-Li Zhang, Yuan-Yuan Pan, Alain Rives, Yan-An Liu, Ling Wei, Zi-Feng Yan

Isobutane dehydrogenation over high-performanced sulfide V-K/γ-Al_2O_3 catalyst: modulation of vanadium species and intrinsic effect of potassium

Yu-Peng Tian[1,2], Xin-Mei Liu[2,*], Svetlana Mintova[2,3], Long-Li Zhang[1], Yuan-Yuan Pan[2,4,*], Alain Rives[5], Yan-An Liu[2], Ling Wei[2], Zi-Feng Yan[2]

[1] *College of Science, China University of Petroleum, Qingdao 266580, China*

[2] *State Key Laboratory of Heavy Oil Processing, China University of Petroleum, Qingdao 266580, China*

[3] *Laboratoire Catalyse et Spectrochimie, ENSICAEN, Université de Caen, 14000, Caen, France*

[4] *College of Chemical Engineering, China University of Petroleum, Qingdao 266580, China*

[5] *Univ. Lille - UMR 8181 CNRS, Centrale Lille, ENSCL, Univ. Artois- UCCS - Unité de Catalyse et de Chimie du Solide, F-59000 Lille, France*

* Corresponding author.

Xin-Mei Liu. Tel: +86-532-86983536. Fax: +86 532 86981787. *E-mail address: lxmei@upc.edu.cn.*

Yuan-Yuan Pan. Tel: +86-532-86981317. *E-mail address: yuanyuanpan@upc.edu.cn.*

Abstract

Compared with industrial used Pt- and Cr-based catalyst in dehydrogenation (DH) of light alkanes, the sulfide V-K/γ-Al_2O_3 catalyst reported in this study shows lower cost and toxicity, and significant DH performance. The yield to isobutene reached as high as 52.9%, which is among the highest reported to date. We attribute such high isobutene yield to the precise modulation of polymerization degree for vanadium species via doping of potassium and indicating that the synergy between vanadium species and acid sites is critical to enhance the DH performance. Our previous work showed sulfidation promoted the increase of DH performance for vanadium-based catalyst, and we go further in this study to explore the correlation between increased range of DH performance and the added potassium. The different loaded potassium leads to variation in sulfidation degree, affecting the properties of vanadium species and acid properties consequently. The potassium was distributed uniformly on surface of the sulfide vanadium-based catalyst and was predominantly bonded with the vanadium species rather than with the γ-Al_2O_3 support. With increasing the potassium amount from 0 to 3 wt.%, the acid amount kept decreasing, and some specific strong acid sites appeared once adequate sulfur was introduced in the V-K/γ-Al_2O_3 catalyst. The characterization and DFT results both revealed that the doped potassium contributes to regulating the vanadium species in the oligomeric state. The synergy between vanadium species and acid properties was regulated by the added potassium simultaneously, and thus the DH performance was enhanced. This study provides promising strategy for preparation of

environment-friendly model industrial DH catalyst.

Keywords: isobutane dehydrogenation, modulation, vanadium species, potassium, intrinsic effect.

1. Introduction

Light alkenes have been widely used as building blocks in chemical industry to produce various important compounds including polypropylene, propylene oxide, butyl rubber, methyl methacrylate, and so on. In comparison with the low-selectivity and energy-inefficient conventional methods like fluid catalytic cracking (FCC) and steam cracking of oil byproducts, dehydrogenation (DH) of light alkanes is becoming an attractive on-purpose and environmental friendly process to produce light alkenes [1-4]. Although Pt- and Cr- based catalysts have been applied in commercial DH processes, the high-cost and environmental concerns restricted their further application. While, vanadium-based catalysts are attracting ever-increasing attention in the DH of alkanes due to the lower cost, less environmental issues and considerably high activity [5-8]. Besides, the vanadium-based catalysts reduce risks to environment and human health.

To modify the structure of DH catalysts and to enhance the DH performance, various promoters were introduced in. Sn was commonly added in Pt-based catalysts, and its promoting effect on both geometric and electronic aspects was extensively studied [1, 9-11]. It was reported that the Sn additives led to creation of smaller Pt ensembles by formation of Pt-Sn alloy and/or partial coverage of Pt. Besides, the electron density of Pt increased after the electrons transferred from tin to platinum atoms. Consequently, the structure-sensitive

side reactions like coking and hydrogenolysis were inhibited, and the olefins easily desorbed from the surface of Pt-based catalysts. The Sn increased the selectivity to olefins, while the conversion of alkanes decreased. The DH activity of Cr-based catalysts was known to be influenced by alkali metals, but the promoting role of alkali metals is still under debate [12-15]. The alkali metal promoters could assist the formation of CrO_3 complexes which transformed to catalytically active Cr_2O_3 under reducing atmosphere [12, 13]. The acidity of Cr-based catalyst was also modified, which inhibited side reactions like cracking and isomerization. The activity and selectivity to product alkenes were consequently promoted. On the other hand, Cavani et al. reported that the potassium added in the Cr/Al_2O_3 catalyst led to the formation of potassium chromate, which consumed the dispersed Cr^{3+} active species [14, 15]. The DH activity of isobutane was generally inhibited by the added potassium. The potassium was also doped in vanadium oxide catalysts to modify the structure and properties [16-19]. It was indicated that the terminal V=O bond was weakened [16, 17]. The acid-base characteristic of the system was changed, which accounted for better selectivity in propane ODH. However, the selectivity to propene increased at the expense of propane conversion [16, 18, 19].

In our previous study, sulfur was first introduced in oxide vanadium-based DH catalysts, and the DH performance was promoted remarkably. Different increased range of DH performance was observed after sulfidation, however, what influence the increased range remains to be determined [20]. Besides, the oligomeric vanadium species were also proven to present the highest DH activity [6, 20]. How to modulate the vanadium species at the

oligomeric state in the complicated sulfide system are yet challenging subjects.

Based on the above issues, we report on the precise modulation of DH performance and polymerization degree for vanadium species via doping of potassium in this study. The intrinsic effect of potassium on synergy between vanadium species and acid sites was also investigated deeply. The added potassium was generally considered to elevate the selectivity to product alkenes, however, the DH activity was inhibited simultaneously [16, 18, 19]. Still the challenge in this study is to maintain the DH activity at a high level after the addition of potassium. The ultimate goal is to prepare an ideal environment-friendly DH catalyst with both high yield and selectivity to isobutene.

2. Experimental section

2.1 Preparation of catalyst

A series of V-K/γ-Al_2O_3 catalysts with the same amount of vanadium (13.5 wt.%) were prepared by incipient wetness impregnation. Initially, NH_4VO_3 (Alfa Aesar Chemical Co. Ltd., 99.9% purity) was dissolved in an aqueous solution of oxalic acid (Sinopharm Chemical Reagent Co. Ltd., 99.5% purity), with a molar ratio of 1:2. Then different amount of KNO_3 (Sinopharm Chemical Reagent Co. Ltd., 99.0% purity) was added into the former solution that serves as a precursor of potassium. Pseudo-boehmite (Zibo Lituo Composite Co. Ltd.) was subsequently impregnated with the solution under mechanically stirring. Finally, the mixture was dried in water bath at 70 °C for 4h, and then kept in oven at 120 °C for 12h. The calcination of the catalyst was conducted at 550 °C for 10h in air with a heating rate of

2 °C/min. For further catalytic evaluation, the as-prepared catalysts were pelleted, crushed and sieved with 20-60 mesh. As for the preparation of sulfide V-K/γ-Al_2O_3 catalysts, the oxide catalysts were pre-sulfided at 560 °C for 3h in a 5% H_2S/H_2 gas with a flow rate of 30 mL/min. The catalysts after sulfidation are denoted as *x*K-S, where "*x*%" is the nominal K_2O content by weight.

2.2 Characterization

XRD measurements were performed using an X'Pert PRO MPD diffractometer, equipped with Cu Kα radiation (40 kV, 40 mA). Raman spectra were recorded on a Thermo Fisher Scientific DXR Raman spectrophotometer at ambient conditions with an excitation wavelength of 532nm. N_2 adsorption–desorption isotherms were recorded with a Quantachrome Autosorb iQ3 Gas Sorption Analyzer at liquid nitrogen temperature. The as-prepared catalysts were outgassed at 300 °C for 4h to remove the adsorbed impurities. The morphology of sulfide vanadium-based catalyst was examined with a JEOL JSM-7900F scanning electron microscope (SEM), and the distribution of the elements was measured by EDS-SEM using JEOL-7900F SEM equipped with an Oxford Instruments X-MaxN Energy-Dispersive Spectroscopy. The FT-IR spectra were recorded on a Nicolet 6700 spectrometer. The samples were put in the atmosphere of pyridine for adsorption with 24h, then the physisorbed pyridine desorbed under vacuum at 150 °C for 2h. The spectra were collected by accumulating 64 scans at a 4 cm^{-1} resolution. NH_3-TPD was conducted on a Micromeritics Autochem 2920 apparatus. During the NH_3-TPD test, the samples (0.1g) were pretreated in a helium flow at 600 °C for 1h, and then the NH_3 was adsorbed on samples at

70 °C for 0.5h. After the adsorption, the gas was switched to helium and the physisorbed NH_3 was desorbed at 110 °C for 0.5h. The temperature then increased to 700 °C with a ramp of 10 °C/min. The NH_3-TPD signal was recorded with a TCD detector. Afterwards, the calibration between the desorption peak area and various concentration of NH_3 was performed on the same apparatus. The acid content was calculated according to this standard curve. XPS was conducted on a Thermo Fisher ESCALAB 250 spectrometer with a monochromatic Al Kα source. The pass energy was 20eV, and the energy step size was set to be 0.05eV. The XPS spectra were obtained under CAE mode operation, meaning that both the energy resolution and pass energy remain constant during the scan. The binding energy of C1s at 284.8 eV for adventitious carbon was adopted as the energy reference.

2.3 Catalytic evaluation

The DH activity was evaluated at atmospheric pressure and at 610 °C in a conventional bench-scale fixed-bed reactor. Typically, 1.0 g of the catalyst with a 20-60 mesh size was loaded in a stainless steel tubular reactor with an internal diameter of 10 mm and a length of 500 mm. As for the catalytic evaluation of sulfide vanadium-based catalysts, the as-prepared oxide catalyst was first heated to 560 °C in 60min under N_2 with a flow rate of 20 mL/min. The gas was then switched to 5% H_2S/H_2 of 30 mL/min, and kept for 3h at 560 °C. Subsequently, the temperature was elevated to 610 °C, and the H_2/isobutane with a volume ratio of 4:1 was introduced. The composition of products was analyzed online with an Agilent 7820A GC equipped with a flame ionization detector and a column of Al_2O_3. The conversion

of isobutane, selectivity to isobutene, and yield to isobutene were determined as follows:

(1) Conversion of isobutane = **Erreur !**

(2) Selectivity to isobutene = **Erreur !**

(3) Yield to isobutene = **Erreur !**

2.4 DFT calculations

The Vienna Ab initio Simulation Package (VASP) was used for the density functional theory (DFT) calculations of the V-clusters [21, 22]. The geometry optimizations were performed with the projector augmented wave (PAW) pseudopotential and the plane-wave basis set with the cut-off energy of 500 eV [23]. Generalized gradient approximation with the Perdew-Burke-Ernzerhof (PBE) form was used for the exchange-correction functional [24]. The Hubbard+U correction was used to describe the electronic on-site coulombic interactions of V 3d orbital with the value of U = 3.2eV [25]. Because periodic boundary condition was used in VASP, the vacuum buffer spaces in three directions were set at least 12 Å. Atomic structures were fully optimized until the forces were smaller than 0.02 eV/Å and the energy was converged to less than 10^{-5} eV between two iteration steps.

It is known that all the vanadium species exist in V^{4+} state during the preparation process of catalysts due to the formation of the complex. The VO_4H_4 model was constructed to represent the vanadium species in the preparation process. Besides, the vanadium loaded was 13.5 wt.% in this study, which mainly exist in polymeric state according to previous studies [6, 26]. It is commonly accepted that polymeric vanadium clusters involve three to five

vanadium atoms [27]. The pentamer $V_5O_xH_y$ species were adopted in this DFT calculation. The valence state of vanadium species also influenced the structure of vanadium species. XPS was conducted to confirm the valence state of vanadium and the V2p XPS spectra were deconvoluted (Fig. S1). It is demonstrated that the average oxidation state was about 4.0.

3. Results and Discussion

3.1 Modulating vanadium species via potassium

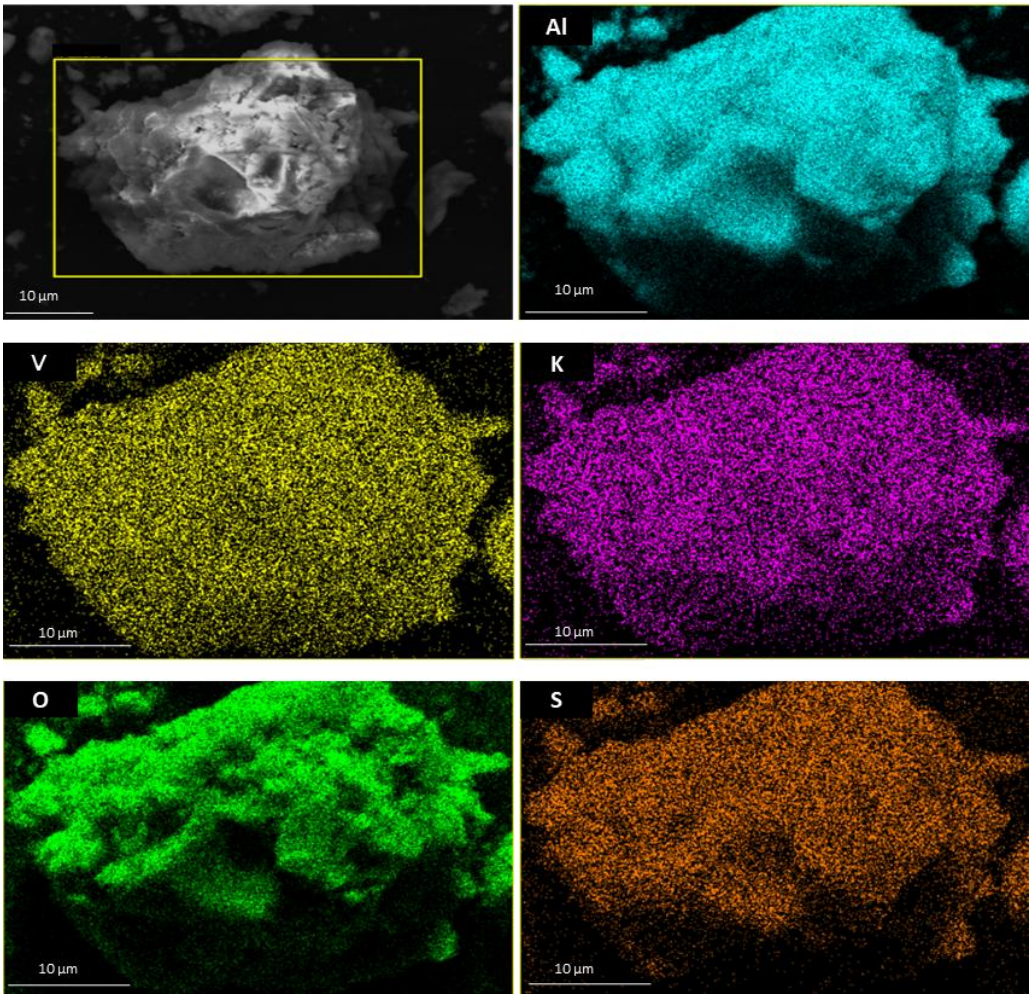

Fig. 1 EDS-SEM images of sample 2.25K-S.

To realize the modulation of vanadium species by the doped potassium, it is crucial to determine the existing form and bonding mode of potassium. EDS-SEM mapping was

performed to reveal the elements' distribution in sample 2.25K-S (Fig. 1). The results show that both potassium and vanadium are distributed uniformly on sample 2.25K-S and no obvious aggregation of specific species is observed. The potassium species might combine with the Al_2O_3 support and/or vanadium species that require further experiments to determine the bonding mode.

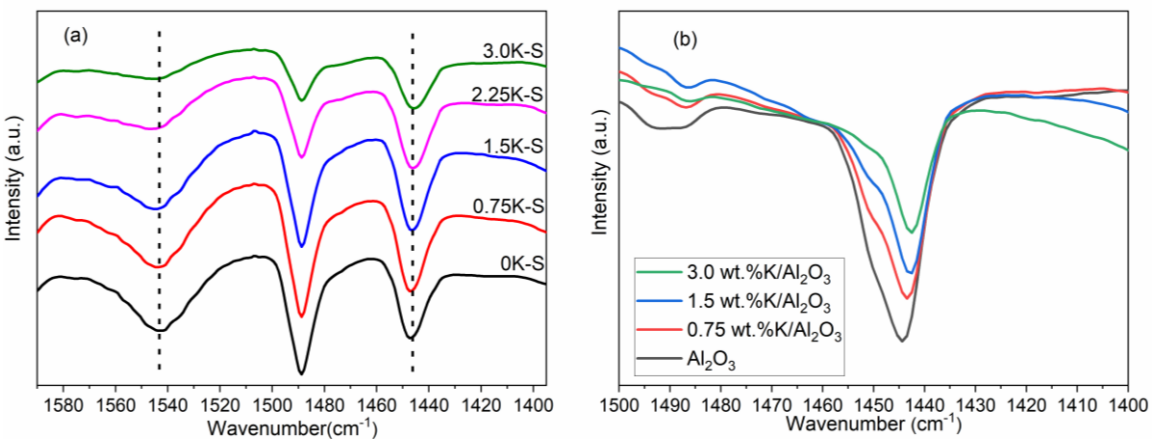

Fig. 2 Py-FT-IR spectra of sulfide V-K/γ-Al_2O_3 catalysts (a) and K/γ-Al_2O_3 samples (b) with different loading amount of potassium.

As a traditional alkaline metal, the potassium would influence the acid properties of the catalysts directly, and the distribution of potassium can be inferred by analyzing the variation of acid properties. The acid type of sulfide vanadium-based catalysts was studied by FT-IR using pyridine as a probe molecule (Fig. 2-a). Two bands at ~1542 and ~1445 cm^{-1} are present in the spectra of all samples and they are attributed to the pyridine adsorbed on Brønsted and Lewis acid sites, respectively. The band at ~1490 cm^{-1} is assigned to pyridine co-adsorbed on both Lewis and Brønsted acid sites. It is commonly accepted that Lewis acid sites on V/γ-Al_2O_3 catalysts mainly originate from coordinative unsaturated Al^{3+} species and/or V^{3+}/V^{4+} species, while the Brønsted acid sites arise from V-OH groups [3, 28, 29].

With potassium increase from 0 to 3 wt. %, the number of Lewis acid sites (NLS) changes very little while the number of Brønsted acid sites (NBS) decreases visibly.

Additionally, different amount of potassium was directly loaded on bare γ-Al_2O_3 support, and the Py-FT-IR spectra of K/γ-Al_2O_3 samples are shown in Fig. 2-b. The peak at ~1445 cm^{-1}, which is attributed to the adsorption of pyridine on Lewis acid sites, is observed for all samples. With increasing the potassium loading, the NLS is decreasing in comparison with the pure γ-Al_2O_3. It is indicated that potassium could combine with γ-Al_2O_3 support directly in the case of no vanadium, resulting in the NLS decrease. As Fig. 2-a shows, the NLS of sulfide V-K/γ-Al_2O_3 catalysts changes little while the NBS decreases obviously with the increase of potassium. The above discussions jointly revealed that the potassium was inclined to combine with vanadium species rather than with γ-Al_2O_3 in V-K/γ-Al_2O_3 catalysts.

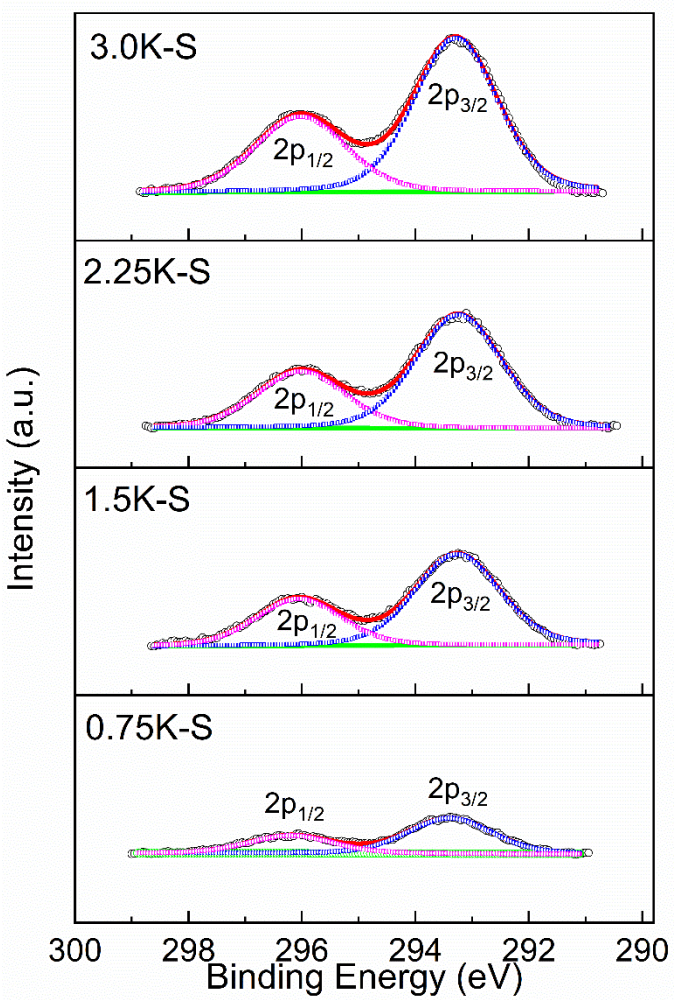

Fig. 3 Peak deconvolution for K2p XPS spectra of sulfide V-K/γ-Al_2O_3 catalysts with different amounts of potassium.

To further understand the bonding mode of potassium, the XPS analysis of the samples was carried out. The K2p XPS spectra for all samples are shown in Fig. 3. The peaks at binding energies of 293.1 eV and at 296.0 eV correspond at the $K2p_{3/2}$ and $K2p_{1/2}$ levels respectively and could be ascribed to K^+ in potassium oxide [30, 31]. The K2p XPS and Py-FT-IR results jointly revealed that the potassium would bond with Brønsted acidic (V-OH) sites, which resulted in the formation of V-O-K/V-S-K bonds.

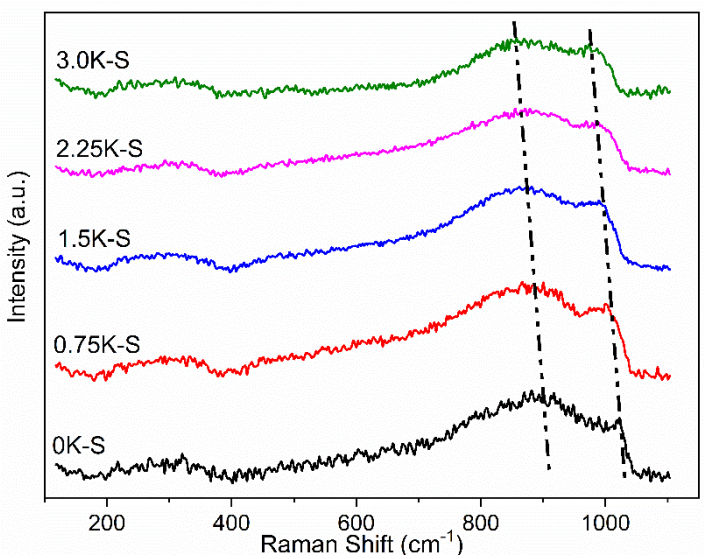

Fig. 4 Raman spectra of sulfide V-K/γ-Al_2O_3 catalysts with different amounts of potassium.

The bond between V and K made it possible to modulate the vanadium species via doping of appropriate potassium. Raman spectra were measured to reveal the influence of potassium on the vanadium species. As shown in Fig. 4, two bands at around ~1050 cm^{-1} and ~900 cm^{-1} are observed, which are attributed to V=O/S and V-O-Al/V-S-Al vibrations, respectively [32, 33]. With the amount of potassium increased, the two characteristic Raman bands shift to lower wavenumbers. The red-shift of the V=O bands is a signature for decrease of polymerization degree of vanadium species [34, 35].

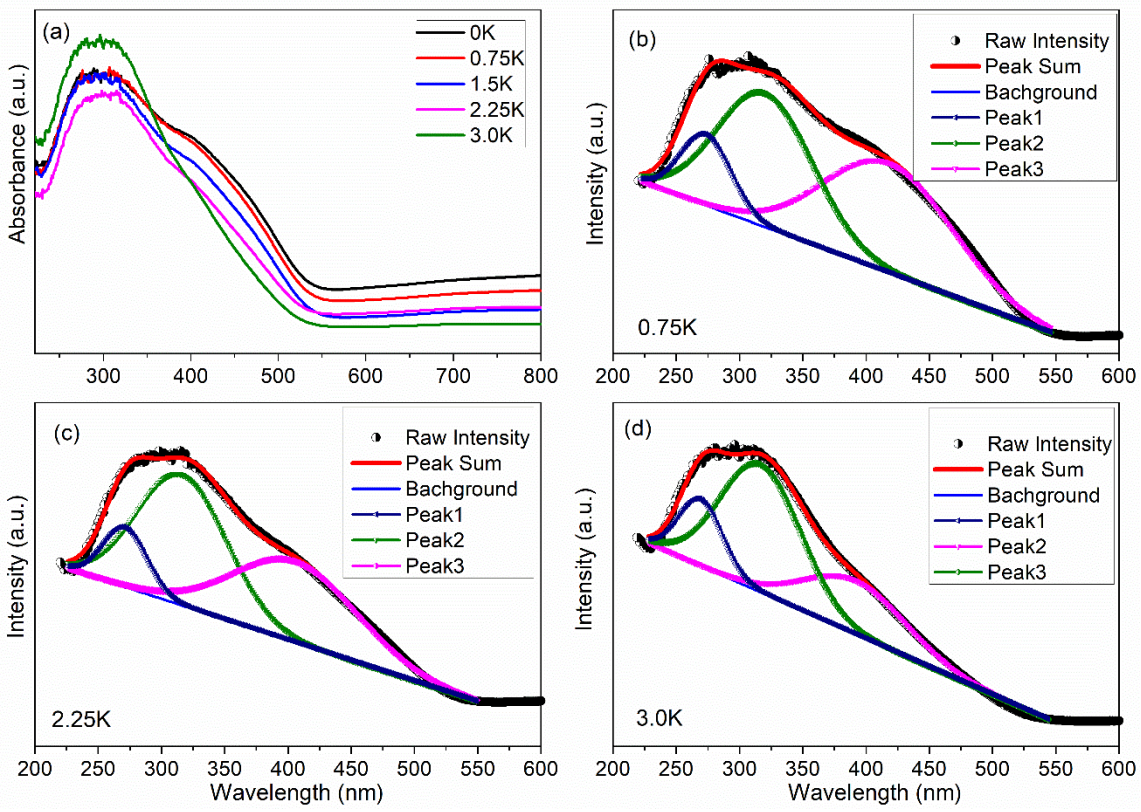

Fig. 5 Diffuse reflectance UV-vis spectra of V-K/γ-Al_2O_3 catalysts with different amounts of potassium (a), and peak deconvolution results for corresponding samples (b-d).

Diffuse reflectance UV-vis spectra of V-K/γ-Al_2O_3 catalysts were also recorded to show the specific changes in polymerization of vanadium species (Fig. 5). Two characteristic bands, including a broad band centered at ~300 nm and the other band at ~420 nm, could be observed for all the samples. After peak deconvolution, three peaks located at ~270 nm (Peak1), ~315 nm (Peak2) and ~420 nm (Peak3) were clearly shown for corresponding samples in Fig. 5(b-d), and the detailed deconvolution results were summarized in Table S1. It is commonly accepted that Peak1 and Peak2 are characteristic for monomeric and oligomeric vanadium species, while Peak3 corresponds to vanadium species with higher polymerization degree [36-38]. According to Table S1, as the potassium content increased, a progressive shift of Peak3 from 417.2nm to 391.1nm is observed, and the relative content of

Peak3 also decreases from 46.3% to 29.2%. Meanwhile, the content of Peak2 increases from 41.9% to 55.1%. Obviously, the vanadium species transformed into oligomeric state progressively. The coherent Raman and UV-vis results reveal that the polymerization degree of vanadium species can be modulated gradually.

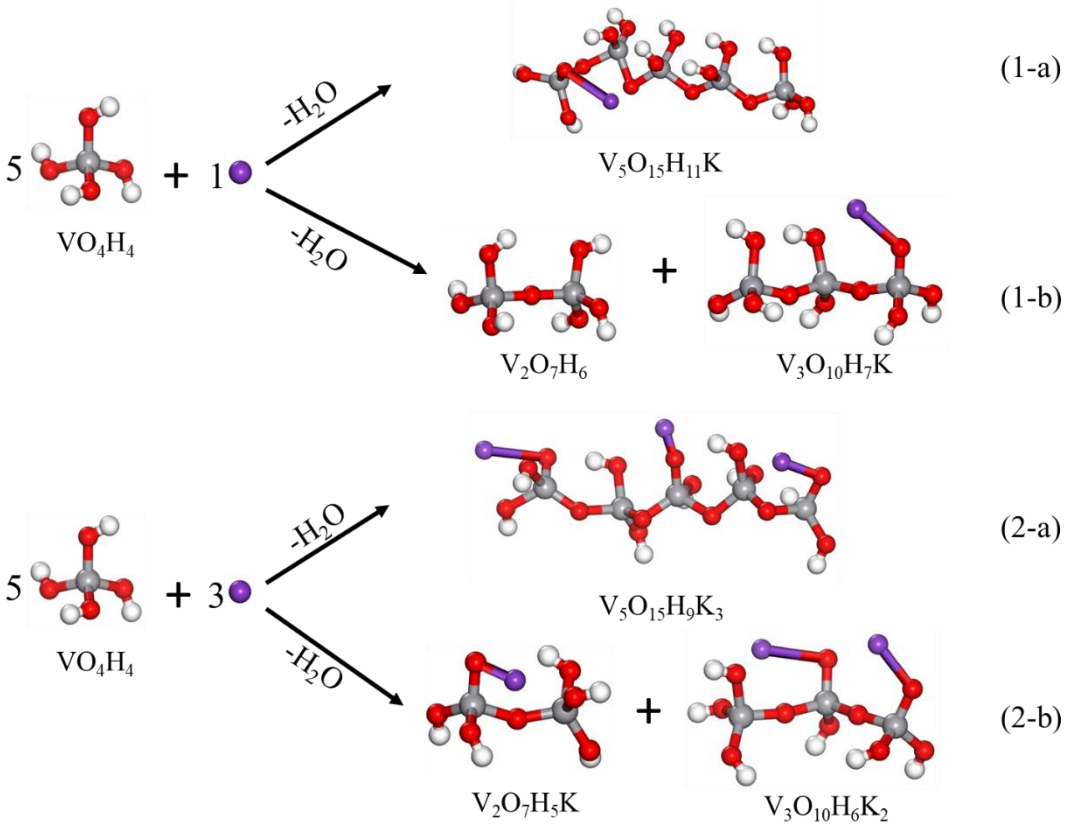

Fig. 6 Schematic illustration of the transforming of VO_4H_4 into either $V_5O_xH_y$ species or V3-cluster and V2-cluster with different K atoms. The gray, red, white, and purple balls represent the V, O, H, and K atoms, respectively.

To further understand the modulation of vanadium species by doped potassium, DFT calculations were performed. The vanadium species in this study actually are present as oxy-sulfide species after pre-sulfidation, due to the special oxophilic character of vanadium oxide species [39-41]. For convenience, vanadium atoms were assumed to bond with oxygen only for the DFT calculations. During the preparation process of the catalysts, the VO_4H_4

species were assumed to form either $V_5O_xH_y$ species, or trimer and dimer clusters. Different amount of potassium was introduced during the formation processes, and the process is schematically illustrated in Fig. 6. The energy change during the formation process were calculated, as defined as $\Delta E = E_{product} - E_{reactant}$ (for more details concerning the calculation of ΔE see Supporting Information).

According to the DFT calculations, $\Delta E_{1\text{-a}}$ and $\Delta E_{1\text{-b}}$ are 35.8 eV and 29.5 eV, respectively. After the potassium atoms were increased to be three, $\Delta E_{2\text{-a}}$ and $\Delta E_{2\text{-b}}$ are calculated to be 55.9 eV and 24.4 eV. As shown, $\Delta E_{1\text{-b}}$ is lower than $\Delta E_{1\text{-a}}$, and $\Delta E_{2\text{-b}}$ is also lower than $\Delta E_{2\text{-a}}$. It indicates that the VO_4H_4 species are easier to transform into trimer and dimer clusters than pentamer vanadium species after potassium was added. Furthermore, $\Delta E_{2\text{-b}}$ is lower than $\Delta E_{1\text{-b}}$, confirming that the increased potassium content is beneficial for the formation of trimer and dimer clusters. The DFT results clarify that potassium decreases the polymerization degree of vanadium species, and the polymerization degree keeps decreasing with increasing the amount of potassium. The DFT data are consistent with the experimental results, further confirming that the vanadium species can be modulated by the doped potassium.

3.2 Effect of potassium on textural and acid properties

The doped potassium contributes to modulate the vanadium species. Simultaneously, the potassium would also influence acid and textural properties of sulfide V-K/γ-Al_2O_3 catalyst. The XRD patterns of samples with different potassium amount were measured, and the effect of potassium on the dispersion of vanadium species was evaluated (Fig. S2). All samples

show three peaks at 36.7°, 45.7° and 66.5°, which are characteristic of γ-Al_2O_3 and consistent with the database standard (JCPDS No. 10-0425). This indicates that the added potassium does not cause aggregation of active vanadium species and formation of new phases.

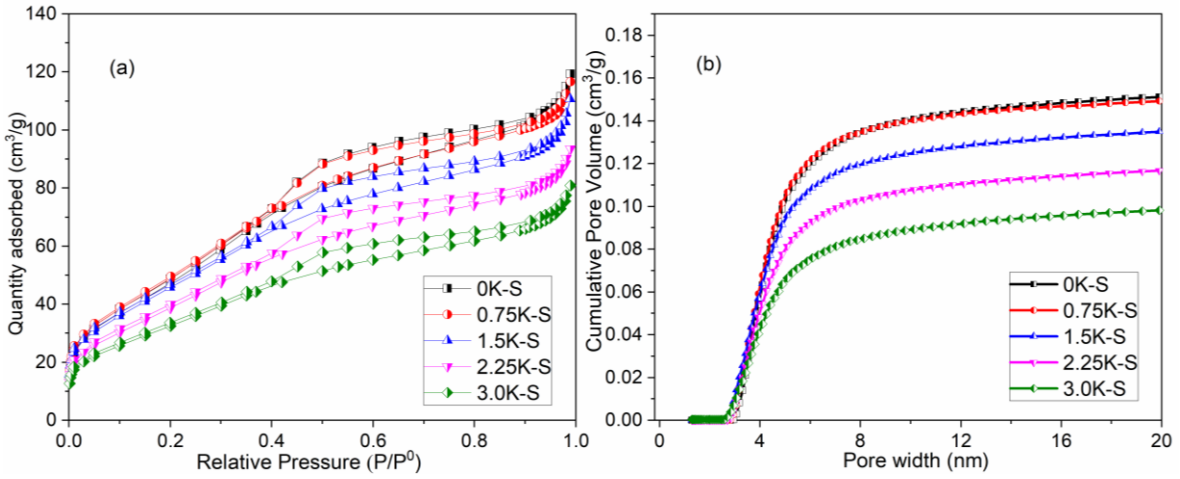

Fig. 7 N_2 adsorption-desorption isotherms (a) and pore size distribution (b) of sulfide V-K/γ-Al_2O_3 catalysts with different amounts of potassium.

Table 1. Catalytic performance and physicochemical properties of different samples.

Sample	S_{BET} ($m^2\ g^{-1}$)	Vp ($cm^3\ g^{-1}$)	Pore Width (nm)	Acid content (μmol g^{-1})	$Y_{Isobutene-1h}$ (wt.%)	S/V atomic ratio
0K-S	185	0.15	3.4	290.9	41.2	0.58
0.75K-S	180	0.15	3.4	221.9	50.4	0.64
1.5K-S	174	0.13	3.3	188.0	52.8	0.69
2.25K-S	143	0.11	3.2	148.9	52.9	0.85
3.0K-S	119	0.09	3.1	63.1	49.8	0.72

N_2 adsorption-desorption isotherms for all catalysts show the influence of potassium on the specific surface area and pore volume (Fig. 7-a). Type IV isotherms were obtained for all samples and the corresponding parameters are summarized in Table 1. With potassium

increasing from 0 to 3 wt.%, the BET surface area decreases from 185.4 (0K-S) to 119.2 m^2 g^{-1} (3K-S). The same trend is also observed for the pore volume (Fig 7-b). The pore volume decreases with increasing the potassium loading, and the pore width is nearly the same. It was demonstrated that potassium causes collapse of the pore structure, which resulted in a decrease of both BET surface area and pore volume of catalysts [42, 43].

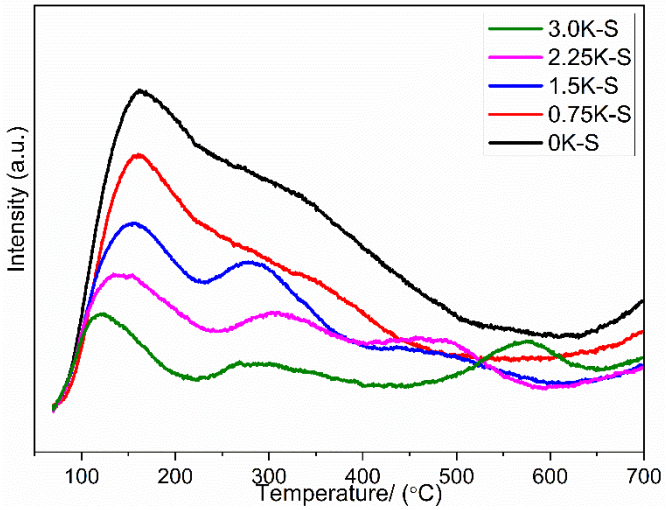

Fig. 8 NH_3-TPD profiles of sulfide V-K/γ-Al_2O_3 catalysts with different amounts of potassium.

The variation of acid type for sulfide V-K/γ-Al_2O_3 catalysts has already been illustrated in Fig. 2-a. With potassium increase from 0 to 3 wt. %, the NLS changes very little while the NBS decreases visibly. Besides, the NH_3 temperature-programmed desorption (NH_3-TPD) was applied to show the effect of potassium on acid content and strength. As can be seen from the NH_3-TPD profiles in Fig. 8, the acid amount keeps decreasing with an increase of potassium loaded. The acid amount decreases from 290.9 μmol/g (0K-S) to 63.1 μmol/g (3.0K-S) (Table 1). The peaks presented below 400 °C are attributed to the desorption of NH_3 from the weak and medium-strong acid sites of the catalysts. The strength of these two kinds of acid sites decreased as the potassium increased. Some specific peaks above 400 °C emerged for samples 1.5K-S, 2.25K-S and 3.0K-S, which originate from the desorption of

NH_3 from strong acid sites. In our previous work, it had been confirmed that the ionicity of V-S bonds is enhanced in comparison to that of V-O due to the lower electronegativity of sulfur, resulting in stronger interaction between VS_x species and NH_3 probe molecule [20]. For samples 1.5K-S, 2.25K-S and 3.0K-S, the influence of potassium on acid strength gradually emerged after adequate sulfur was introduced in.

3.3 Precise promotion of dehydrogenation performance

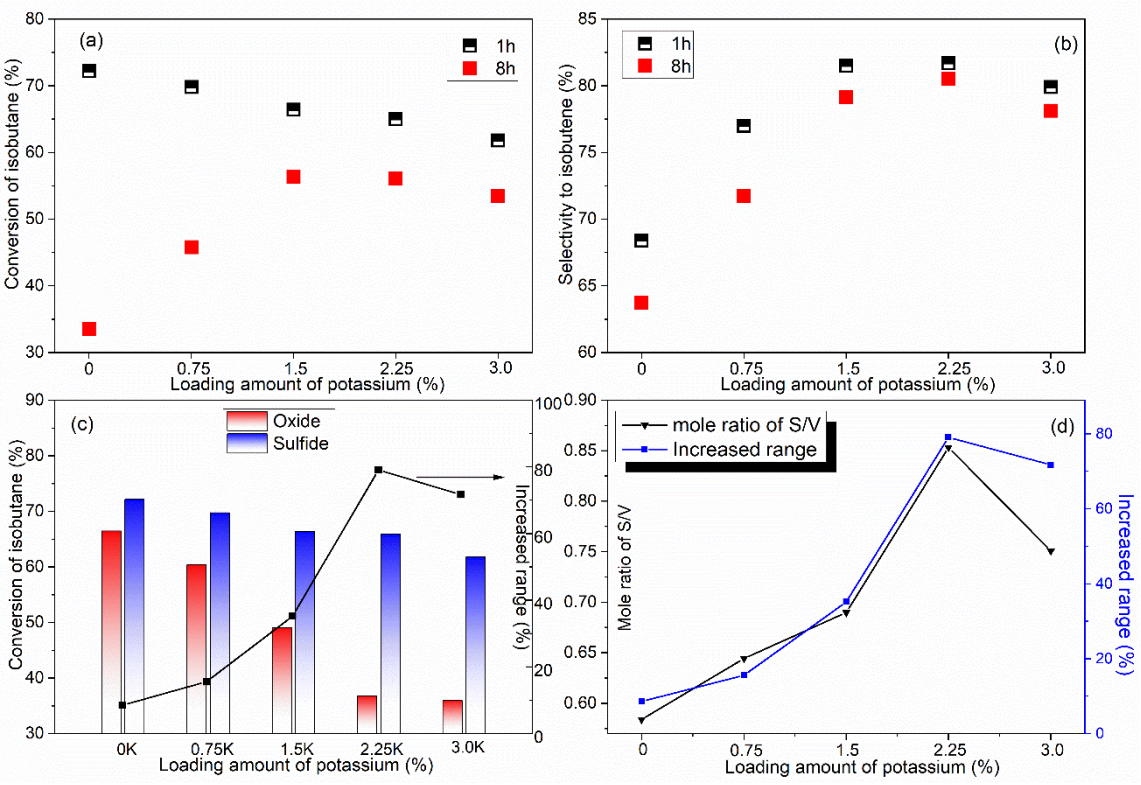

Fig. 9 Evaluation of V-K/γ-Al_2O_3 catalysts with different amounts of K in dehydrogenation reaction: Conversion of isobutane for sulfide catalysts (a), selectivity to isobutene for sulfide catalysts (b), increased range of conversion after sulfidation (c), and correlation between mole ratio of S/V and increased range of conversion (d).

The above discussions show that the synergy between vanadium species and acid properties of vanadium-based catalysts can be influenced by the doped potassium, and the DH performance was affected accordingly. The DH performance for sulfide V-K/γ-Al_2O_3

311 catalysts with different amount of potassium was evaluated using a conventional bench-scale
312 fixed-bed reactor for 8 hours. The DH performance selected at time-on-stream for 1h and 8h
313 is shown in Fig. 9 (a) and (b). With the increase of potassium from 0 to 3 wt.%, the
314 conversion of isobutane decreases from 72.2% (0K-S) to 61.8% (3.0K-S). The selectivity to
315 isobutene reaches as high as ~80% for samples 3K-S, 2.25K-S and 1.5K-S. The yield to
316 isobutene at time-on-stream for 1h is summarized in Table 1, and sample 2.25K-S presents
317 the highest yield to isobutene, reaching up to 52.9%, which is among the best reported to
318 date.

319 The DH performance for corresponding oxide catalysts without pre-treatment by H_2S/H_2
320 was also evaluated. The conversion of isobutane at time-on-stream of 1h for oxide and sulfide
321 V-K/γ-Al_2O_3 catalysts are shown in Fig. 9 (c). The DH performance increases substantially
322 after sulfidation, and increased range of conversion was also calculated. Notably, different
323 amounts of potassium lead to various increased range. The increased range of conversion
324 shows a volcano shape with increasing the potassium loading, reaching a peak for sample
325 2.25K-S. After sulfidation, the conversion of isobutane for sample 2.25K-S increases from
326 36.8% to 65.9%, showing the biggest increased range.

327 Due to the special oxophilic character of vanadium oxide species, it was difficult to get all
328 the oxygen substituted by sulfur via O-S exchange [39-41]. The vanadium species in this
329 study actually are present as oxy-sulfide species after pretreatment by H_2S/H_2. The S2p XPS
330 spectra of samples after treatment with H_2S/H_2 are presented in Fig. S3. It is shown that the
331 majority of introduced sulfur existed in the S^{2-} state, while a little amount of sulfur was

oxidized (SO_4^{2-} species) due to air exposure during the XPS test [44, 45]. We believe that the sulfidation degree might lead to variation in the increased range of conversion. XPS was carried out to characterize the relative atomic ratio of sulfur and vanadium. As the same amount of vanadium was introduced in all samples, the atomic ratio of S/V was calculated to indicate the degree of sulfidation. It is demonstrated in Fig. 9 (d) that the mole ratio of S/V and the increased range of conversion both present volcano curve, reaching a peak for sample 2.25K-S. The correlation between increased range of DH performance and the added potassium was clearly figured out, realizing the precise promotion of DH performance.

As stated above, the polymerization degree of vanadium species kept decreasing with the potassium increasing from 0 to 3 wt.%. It implies that part of the bridge bonds between vanadium ions broke down and consequently new chemical bonds between vanadium ion and Al_2O_3 support are formed. Thus replacing oxygen by sulfur during the pre-sulfidation treatment is becoming more difficult. Meanwhile, the increasing alkaline potassium would react with H_2S to attract more sulfur to introduce. The combined effect is exemplified as a volcano curve of sulfidation degree with potassium increase from 0 to 3 wt.% (Fig 9-d). It is obvious that the different loading amount of potassium leads to variation in sulfidation degree, affecting the vanadium species and acid properties ultimately.

4.Conclusions

This study reports on the precise modulation of vanadium species and DH performance via the doped potassium with a simple coimpregnation process. It is also shown that the synergy

between vanadium species and acid sites plays a critical role in enhancing DH activity. Ultimately, the yield to isobutene over sulfide V-K/γ-Al_2O_3 catalysts reached as high as 52.9%, which is among the highest reported to date.

Combining characterization and DFT results, we revealed that the potassium was predominantly bonded with the vanadium species, and the polymerization degree of vanadium species depends significantly on the potassium. The doped potassium contributes to regulating the vanadium species in the oligomeric state. Simultaneously, the bond between K and Brønsted acidic (V-OH) species would also influence the sulfidation degree and acid strength of V-K/γ-Al_2O_3 catalysts. The intrinsic effect of potassium on synergy between vanadium species and acid sites promotes the enhancement of DH activity obviously. This study provides promising strategy for preparation of environment-friendly model industrial DH catalyst.

Conflicts of interest

There are no conflicts of interest to declare.

Acknowledgements

This work was financially supported by the National Natural Science Foundation of China (22008261, 21978326), the Key Technology Research and Development Program of Shandong Province (ZR2019MB029), the Fundamental Research Funds for the Central Universities (20CX06062A, 20CX06059A), and the Postdoctoral Applied Research Project

374 of Qingdao (qd20200005).

375

Reference

[1] J.J. Sattler, J. Ruiz-Martinez, E. Santillan-Jimenez, B.M. Weckhuysen, Catalytic dehydrogenation of light alkanes on metals and metal oxides, Chem. Rev. 114 (2014) 10613-10653.

[2] T. Otroshchenko, G.Y. Jiang, V.A. Kondratenko, U. Rodemerck, E.V. Kondratenko, Current status and perspectives in oxidative, non-oxidative and CO_2-mediated dehydrogenation of propane and isobutane over metal oxide catalysts, Chem. Soc. Rev. 50 (2021) 473-527.

[3] U. Rodemerck, M. Stoyanova, E.V. Kondratenko, D. Linke, Influence of the kind of VO_x structures in VO_x/MCM-41 on activity, selectivity and stability in dehydrogenation of propane and isobutane, J. Catal. 352 (2017) 256-263.

[4] N. Kaylor, R.J. Davis, Propane dehydrogenation over supported Pt-Sn nanoparticles, J. Catal. 367 (2018) 181-193.

[5] Z.G. Fan, T.Q. Zeng, W.H. Wu, D.Y. Jiang, C.X. Miao, Dehydrogenation of isobutane to isobutene over isolated VO_x-species on MCM-41 under oxygen-lean conditions, Ind. Eng. Chem. Res. 58 (2019) 10249-10254.

[6] Y.-P. Tian, P. Bai, S.-M. Liu, X.-M. Liu, Z.-F. Yan, VO_x–K_2O/γ-Al_2O_3 catalyst for nonoxidative dehydrogenation of isobutane, Fuel Process. Technol. 151 (2016) 31-39.

[7] V.P. Vislovskiy, N.T. Shamilov, A.M. Sardarly, V.Y. Bychkov, M.Y. Sinev, P. Ruiz, R.X. Valenzuela, V. Cortés Corberán, Improvement of catalytic functions of binary V-Sb oxide catalysts for oxidative conversion of isobutane to isobutene, Chem. Eng. J. 95 (2003) 37-45.

[8] A. Rodriguez-Gomez, A.D. Chowdhury, M. Caglayan, J.A. Bau, E. Abou-Hamad, J. Gascon. Non-oxidative dehydrogenation of isobutane over supported vanadium oxide: nature of the active sites and coke formation. Catal. Sci. Technol. 10 (2020) 6139-6151.

[9] G. Wang, H. Zhang, H. Wang, Q. Zhu, C. Li, H. Shan, The role of metallic Sn species in catalytic dehydrogenation of propane: active component rather than only promoter, J. Catal. 344 (2016) 606-608.

[10] L.G. Cesar, C. Yang, Z. Lu, Y. Ren, G. Zhang, J.T. Miller, Identification of a Pt3Co

Surface Intermetallic Alloy in Pt-Co Propane Dehydrogenation Catalysts, ACS Catal. (2019) 5231-5244.

[11]X.P. Wu, Q. Zhang, L.G. Chen, Q.Y. Liu, X.H. Zhang, Q. Zhang, L.L. Ma, C.G. Wang, Enhanced catalytic performance of PtSn catalysts for propane dehydrogenation by a Zn-modified Mg(Al)O support, Fuel Process. Tech. 198 (2020) 106222-106231.

[12] T.P. Otroshchenko, U. Rodemerck, D. Linke, E.V. Kondratenko, Synergy effect between Zr and Cr active sites in binary $CrZrO_x$ or supported $CrO_x/LaZrO_x$: Consequences for catalyst activity, selectivity and durability in non-oxidative propane dehydrogenation, J. Catal. 356 (2017) 197-205.

[13] H. Zhao, H. Song, L. Xu, L. Chou, Isobutane dehydrogenation over the mesoporous Cr_2O_3/Al_2O_3 catalysts synthesized from a metal-organic framework MIL-101, Appl. Catal. A Gen. 456 (2013) 188-196.

[14] F. Cavani, M. Koutyrev, F. Trifiro, A. Bartolini, D. Ghisletti, R. Iezzi, A. Santucci, G. Del Piero, Chemical and physical characterization of alumina-supported chromia-based catalysts and their activity in dehydrogenation of isobutane, J. Catal. 158 (1996) 236-250.

[15] E. Rombi, M.G. Cutrufello, V. Solinas, S. De Rossi, G. Ferraris, A. Pistone, Effects of potassium addition on the acidity and reducibility of chromia/alumina dehydrogenation catalysts, Appl. Catal. A Gen. 251 (2003) 255-266.

[16] G. Garcia Cortez, J.L.G. Fierro, M.A. Bañares, Role of potassium on the structure and activity of alumina-supported vanadium oxide catalysts for propane oxidative dehydrogenation, Catal. Today 78 (2003) 219-228.

[17] M. Calatayud, C. Minot, Effect of alkali doping on a V_2O_5/TiO_2 catalyst from periodic DFT calculations, J. Phys. Chem. C 111 (2007) 6411-6417.

[18] C. Resini, M. Panizza, L. Arrighi, S. Sechi, G. Busca, R. Miglio, S. Rossini, A study of the reaction pathway upon propane oxidation over $V\text{-}K/Al_2O_3$ catalysts, Chem. Eng. J. 89 (2002) 75-87.

[19] V. Ermini, E. Finocchio, S. Sechi, G. Busca, S. Rossini, Propane oxydehydrogenation over alumina-supported vanadia doped with manganese and potassium, Appl. Catal. A Gen.

198 (2000) 67-79.

[20] Y.-P. Tian, Y.-A. Liu, X.-M. Liu, Z.-F. Yan, Sulfur introduction in V-K/γ-Al_2O_3 catalyst for high performance in the non-oxidative dehydrogenation of isobutane, Catal. Sci. Technol. 8 (2018) 5473-5481.

[21] G. Kresse, J. Hafner, Ab Initio Molecular Dynamics for Liquid Metals, Phys. Rev. B 47 (1993) 558-561.

[22] G. Kresse, J. Furthmüller, Efficient Iterative Schemes for ab initio total-energy calculations using a plane-wave basis set, Phys. Rev. B 54 (1996) 11169-11186.

[23] G. Kresse, D. Joubert, From ultrasoft pseudopotentials to the projector augmented-wave method, Phys. Rev. B 59 (1999) 1758-1775.

[24] J.P. Perdew, K. Burke, M. Ernzerhof, Generalized gradient approximation made simple, Phys. Rev. Lett. 77 (1996) 3865-3868.

[25] L. Wang, T. Maxisch, G. Ceder, Oxidation energies of transition metal oxides within the GGA+U framework, Phys. Rev. B 73 (2006) 195-207.

[26] G. Liu, Z.-J. Zhao, T. Wu, L. Zeng, J. Gong, Nature of the active sites of VO_x/Al_2O_3 catalysts for propane dehydrogenation, ACS Catal. 6 (2016) 5207-5214.

[27] Z.J. Zhao, T. Wu, C. Xiong, G. Sun, R. Mu, L. Zeng, J. Gong, Hydroxyl-mediated non-oxidative propane dehydrogenation over VO_x/gamma-Al_2O_3 catalysts with improved stability, Angew Chem. Int. Ed. Engl. 57 (2018) 6791-6795.

[28] M. Martínez-Huerta, X. Gao, H. Tian, I. Wachs, J. Fierro, M.A. Banares, Oxidative dehydrogenation of ethane to ethylene over alumina-supported vanadium oxide catalysts: relationship between molecular structures and chemical reactivity, Catal. Today 118 (2006) 279-287.

[29] Y.-P. Tian, X.-M. Liu, M.J. Rood, Z.-F. Yan, Study of coke deposited on a VO_x-K_2O/γ-Al_2O_3 catalyst in the non-oxidative dehydrogenation of isobutane, Appl. Catal. A-Gen. 545 (2017) 1-9.

[30] K.H. Park, B.H. Kim, S.H. Song, J. Kwon, B.S. Kong, K. Kang, S. Jeon, Exfoliation of Non-Oxidized Graphene Flakes for Scalable Conductive Film, Nano Lett. 12 (2012)

460 2871-2876.
461 [31] K.J. Hüttinger, R. Minges, The influence of the catalyst precursor anion in catalysis of
462 water vapour gasification of carbon by potassium: 2. catalytic activity as influenced by
463 activation and deactivation reactions, Fuel 65 (1986) 1122-1128.
464 [32] Z. Wu, P. Stair, UV Raman spectroscopic studies of V/θ-Al_2O_3 catalysts in butane
465 dehydrogenation, J. Catal. 237 (2006) 220-229.
466 [33] C. Zhao, I.E. Wachs, Selective oxidation of propylene to acrolein over supported
467 V_2O_5/Nb_2O_5 catalysts: An in situ Raman, IR, TPSR and kinetic study, Catal. Today 118 (2006)
468 332-343.
469 [34] Z. Wu, H.-S. Kim, P.C. Stair, S. Rugmini, S.D. Jackson, On the structure of vanadium
470 oxide supported on aluminas: UV and visible Raman spectroscopy, UV-visible diffuse
471 reflectance spectroscopy, and temperature-programmed reduction studies, J. Phys. Chem. B.
472 109 (2005) 2793-2800.
473 [35] B. Solsona, T. Blasco, J.M. López Nieto, M.L. Peña, F. Rey, A. Vidal-Moya, Vanadium
474 oxide supported on mesoporous MCM-41 as selective catalysts in the oxidative
475 dehydrogenation of alkanes, J. Catal. 203 (2001) 443-452.
476 [36] Y.-M. Liu, Y. Cao, N. Yi, W.-L. Feng, W.-L. Dai, S.-R. Yan, H.-Y. He, K.-N. Fan,
477 Vanadium oxide supported on mesoporous SBA-15 as highly selective catalysts in the
478 oxidative dehydrogenation of propane, J. Catal. 224 (2004) 417-428.
479 [37] M. Baltes, K. Cassiers, P. Van Der Voort, B.M. Weckhuysen, R.A. Schoonheydt, E.F.
480 Vansant, MCM-48-supported vanadium oxide catalysts, prepared by the molecular designed
481 dispersion of $VO(acac)_2$: a detailed study of the highly reactive MCM-48 surface and the
482 structure and activity of the deposited VO_x, J. Catal. 197 (2001) 160-171.
483 [38] J.L. Male, H.G. Niessen, A.T. Bell, T. Don Tilley, Thermolytic molecular precursor route
484 to active and selective vanadia-zirconia catalysts for the oxidative dehydrogenation of
485 propane, J. Catal. 194 (2000) 431-444.
486 [39] C. Guillard, M. Lacroix, M. Vrinat, M. Breysse, B. Mocaer, J. Grimblot, T. des Courieres,
487 D. Faure, Preparation, characterization and catalytic properties of unsupported vanadium

sulphides, Catal. Today 7 (1990) 587-600.

[40] R.L.C. Bonne, A.D. Vanlangeveld, J.A. Moulijn, Temperature-programmed sulfiding of vanadium oxides and alumina-supported vanadium oxide catalysts, J. Catal. 154 (1995) 115-123.

[41] R. Hubaut, Vanadium-based sulfides as hydrotreating catalysts, Appl. Catal. A Gen. 322 (2007) 121-128.

[42] S.J. Wang, S.F. Yin, L. Li, B.Q. Xu, C.F. Ng, C.T. Au, Investigation on modification of Ru/CNTs catalyst for the generation of CO_x-free hydrogen from ammonia, Appl. Catal. B Environ. 52 (2004) 287-299.

[43] H. Xiong, M.A. Motchelaho, M. Moyo, L.L. Jewell, N.J. Coville, Effect of group I alkali metal promoters on Fe/CNT catalysts in Fischer-Tropsch synthesis, Fuel 150 (2015) 687-696.

[44] L. Qiu, K. Zou, G. Xu, Investigation on the sulfur state and phase transformation of spent and regenerated S zorb sorbents using XPS and XRD, Appl. Surf. Sci. 266 (2013) 230-234.

[45] G. Wang, Z. Meng, J. Liu, C. Li, H. Shan, Promoting effect of sulfur addition on the catalytic performance of Ni/$MgAl_2O_4$ catalysts for isobutane dehydrogenation, ACS Catal. 3 (2013) 2992-3001.